NUCLEATION AND GROWTH OF SILVER NANOPARTICLES MONITORED BY TITRATION MICROCALORIMETRY

R. Patakfalvi[2] and I. Dékány[1,2]*

[1]Department of Colloid Chemistry, University of Szeged, Aradi v. t. 1, H-6720 Szeged, Hungary
[2]Nanostructured Materials Research Group of the Hungarian Academy of Sciences, University of Szeged, Aradi v. t. 1
H-6720 Szeged, Hungary

The nucleation and the growth of silver nanoparticles were studied by spectrophotometry and transmission electron microscopy, with simultaneous recording of the concomitant enthalpy changes. Silver nanoparticles were stabilized by sodium citrate and reduction was brought about by the addition of hydroquinone in aqueous medium. It was established that nucleation is an exothermic process and heat effects are basically determined by the ratio of silver ions to hydroquinone. The process of nanoparticle formation was divided to three phases: the nucleation phase is exothermic, the growth phase is endothermic and further addition of the reducing agent results in the aggregation of silver nanoparticles, which produces a second exothermic heat effect.

Keywords: *aggregation, enthalpy of particle formation, nucleation, silver nanoparticles*

Introduction

The preparation of noble metal nanoparticles has been addressed by numerous studies. The majority of these publications discuss the preparation of nanoparticles by reduction and report the size and the size distribution of particles stabilized by various methods [1–5]. The preparation of silver nanoparticles has an especially voluminous literature, because not only classical colloid chemistry [6, 7] but also modern nanotechnology includes many different procedures for the preparation, the particle size control and the surface modification of Ag nanoparticles [8–11].

The simplest method for the detection of Ag nanoparticles is UV-Vis spectroscopy, because these particles have a characteristic plasmon absorption band of high intensity in the visual range [12]. When the initial concentrations of the precursor, the stabilizing agent and the reducing agent are suitably chosen, the rates of particle formation and growth will be sufficiently slow to be monitored by spectroscopy. Kim *et al*. selected various silver salts and studied the effect of the chemical nature of the precursor on the formation rate of metal nanoparticles [13]. In the presence of $AgBF_4$, $AgPF_6$ and $AgClO_4$ the fast initial reaction rate slowed down after about 10 min, whereas in the case of $AgNO_3$ a slower but constant reaction rate was observed. They attributed this phenomenon to the strong interaction between silver and nitrate ions. The course of the absorbance spectra also allows conclusions to be drawn as

to the size, the size distribution and the aggregation state of nanoparticles [14–16].

The thermodynamical analysis of nanoparticle formation has been undertaken by relatively few studies. The first calorimetric measurements were carried out by Turco Liveri *et al*. in the early nineties [17–20]. They prepared nanoparticles in microemulsions, exploiting the possibility of synthesizing nanoparticles of controlled size within the aqueous droplets of water in oil (*w/o*) microemulsions. They studied the formation of micellar microphases (the reactions of macrocyclic ligands) in Aerosol OT reverse microemulsions [17] and later synthesized palladium nanoparticles in water/AOT/*n*-heptane microemulsions [18]. They established that the energetic states of Pd nanoparticles in microemulsions and in the bulk aqueous phase are entirely different. Their results showed that the heat of formation is a function of particle size and the enthalpy of formation depends on the diameter of the microemulsion droplet. They also established that the duration of nucleation is a few seconds, whereas nanoparticle growth spans a time period of minutes. The enthalpies of formation are exothermic, i.e. particle formation (the reduction of Pd^{2+} ions) is an exothermic process. The extent of exothermicity increases with particle crystal size. The largest heat of formation was measured in pure water (ca. –400 to –500 kJ mol^{-1}). They carried out similar experiments for the preparation of gold nanoparticles in *w/o* microemulsions [19]. As particle size increased, the formation of Au nanoparticles was accompanied by an exothermic heat effect of –246 to

---

–480 kJ mol^{-1}. They showed that there are more atoms on the surface of the nanoparticles than inside them. Therefore, when nanoparticle size decreases, the enthalpy of formation will be a less exothermic process. Thus, when the droplet size of microemulsions is decreased, smaller particles are formed and the process of formation may turn endothermic [19, 20].

Our present work is a calorimetric study of the formation Ag nanoparticles stabilized by Na-citrate molecules. We examined how changes in the concentrations of the Ag$^+$ precursor ions and the reducing agent (hydroquinone) affect the enthalpy of formation.

Materials and methods

Materials used for the preparation of silver sols were: silver nitrate (Reanal, 99.9%), sodium citrate dihydrate (Aldrich, 99%), hydroquinone (*hq*) (Aldrich, 99%).

Microcalorimetry was performed in a Thermal Activity Monitor (TAM 2277) isothermic titration microcalorimeter. AgNO$_3$ and Na-citrate solutions of given concentrations were added to the sample cell in a volume of 2.0 mL. The reducing agent, 10·50 μL of hydroquinone stock solution was next added under constant stirring to the thermostated AgNO$_3$+Na-citrate solution using a programmed automated burette (Lund, Sweden). Enthalpies of mixing arising as a consequence of mixing the given solutions were determined in a separate experiment by adding 10·50 μL of hydroquinone to a solution containing no Ag$^+$ ions. The measurements were controlled and the results (the calorimetric peaks) were evaluated with the help of the DigiTAM 4.1 software.

The reduction of sols was also monitored by UV-Vis spectrophotometry (Uvicon 930 UV-Vis spectrophotometer) in the wavelength range of λ= 300–800 nm. The experimental setup was similar to that of the calorimetric measurements (the measurement volume and the concentrations of the components were identical and spectra were recorded 60 min after the addition of the individual portions of the reducing agent).

Samples were simultaneously withdrawn for transmission electron microscopy (TEM). Transmission electron micrographs were taken in a Philips CM-10 transmission electron microscope with an accelerating voltage of 100 kV. The microscope was equipped with a Megaview II digital camera. The size distribution of the particles was determined by the UTHSCSA Image Tool 3.00 software.

Results and discussion

When hydroquinone was added to the AgNO$_3$ solution filled into the microcalorimeter cell, Ag$^+$ ions were reduced to metallic silver nanoparticles. Reduction changed the colour of the solution and a yellowish-brown Ag sol was formed, whose shade depended on the concentration of silver ions. Na-citrate present in the solution played an important role in the stabilization of the silver colloid particles. If no Na-citrate was added to the solution prior to reduction, the silver particles formed aggregate and precipitate on the bottom of the titration cell. We therefore used 10 mM Na-citrate to stabilize Ag nanoparticles in colloid solution in all cases.

In our experiments the reducing agent hydroquinone was added to AgNO$_3$ solutions of various concentrations in order to observe whether the formation of nanosize silver metal particles was an energetically favoured process. We wished to examine how the amount of heat released or absorbed in the course of reduction changes when the concentration of precursor Ag$^+$ ions is increased. Figure 1a shows the enthalpogram of 4 mM AgNO$_3$ solution during the addition of 10·50 μL of reducing agent ([Ag$^+$]/[hydroquinone]=14). When the reducing agent was added gradually, in hourly portions under constant stirring, increasingly larger endothermic heat effects were ob-
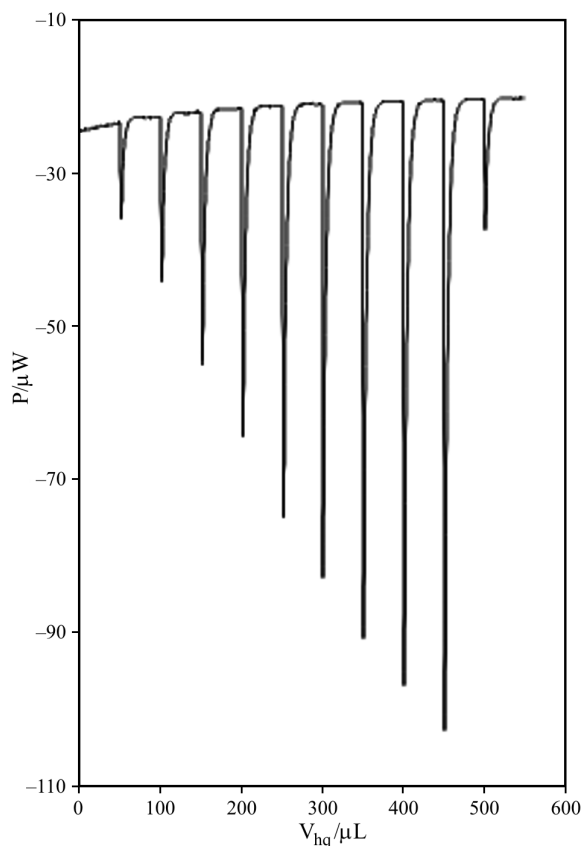

Fig. 1a Typical enthalpogram of the formation of silver nanoparticles, [Ag$^+$]/[hq]=14 (10·50 μL 1 mM hydroquinone solution is added to 1.75 mL 4 mM AgNO$_3$ and 0.25 mL 10 mM Na citrate)
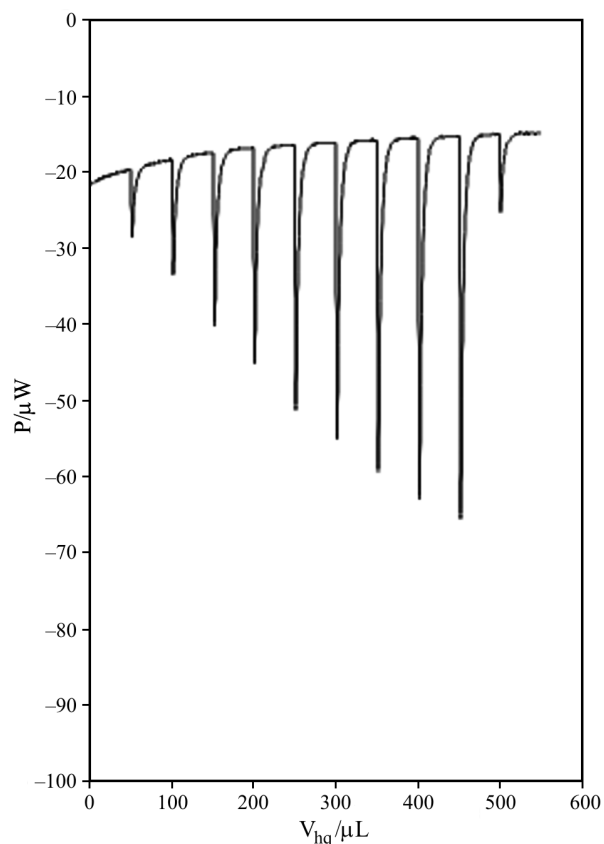
Fig. 1b Typical enthalpogram of the mixing of the components (10·50 μL 1 mM hydroquinone solution is added to 1.75 mL water and 0.25 mL 10 mM Na citrate)

Fig. 2 Enthalpogram of the formation of larger, aggregated nanoparticles, [Ag$^+$]/[hq]=0.875 (10·50 μL 40 mM hydroquinone solution is added to 1.75 mL 10 mM AgNO$_3$ and 0.25 mL 10 mM Na citrate)

served. The enthalpogram of mixing recorded in the absence of Ag$^+$ ions (Fig. 1b) showed that the mixing of the components has even more significant endothermic heat effect than the formation of silver nanoparticles (Fig. 1a demonstrates the heat of mixing and the formation of Ag nanoparticles).

When AgNO$_3$ solution of a higher concentration (e.g. 10 mM) was titrated in the calorimeter with 40 mM hydroquinone ([Ag$^+$]/[hydroquinone]=0.875), exothermic heat effects were obtained already at the initial stages of the experiment (Fig. 2), indicating that at higher concentrations the reduction of Ag$^+$ ions was, on the whole, an exothermic process, in spite of the fact that the heat effect of mixing was endothermic. The total enthalpy changes measured by calorimetry were fulfilled in the following way:

$$\Delta H_{\text{total}} = \Delta H_{\text{nucl}} + \Delta H_{\text{mix}}$$

where ΔH_{nucl} is the enthalpy of particle formation (nucleation) and ΔH_{mix} is the enthalpy of mixing in the reduction (titration) process. When the values of ΔH_{mix} are known from separate measurements, the value of $\Delta H_{\text{nucl}} = \Delta H_{\text{total}} - \Delta H_{\text{mix}}$ can be calculated in every reduction step. After adding these enthalpy values, the integral enthalpy $\Sigma\Delta H_{\text{nucl}} = f(V_{\text{hq}})$ functions showing the
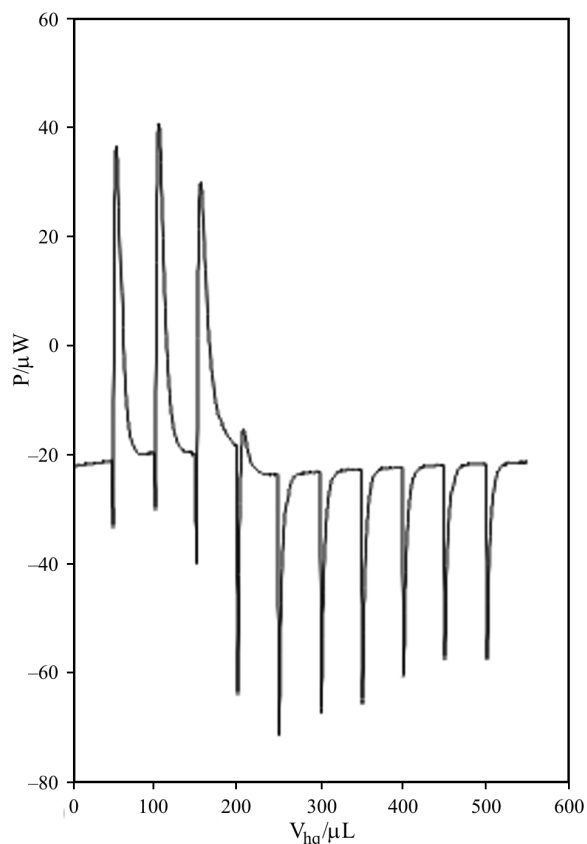
change in enthalpy due to the addition of hydroquinone can be drawn up (Fig. 3). It is clearly seen that if a maximum of 0.5 mL of 1 mM hydroquinone is added to 10 mM Na-citrate solution, the enthalpy of mixing (ΔH_{mix}) brings about a maximally endothermic change in enthalpy, −110 mJ, in the calorimeter. When samples with increasing AgNO$_3$ concentrations were reduced, the integral enthalpy of reduction increased with the addition of hydroquinone; however, the magnitude of the endothermic effects decreased at AgNO$_3$ concentrations of 4, 6 and 8 mM ([Ag$^+$]/[hydroquinone]=14, 21, 28). When 10 mM AgNO$_3$ solution was reduced ([Ag$^+$]/[hydroquinone]=35), the values of the net integral enthalpy of reduction already fell into the exothermic range, indicating that at higher hydroquinone concentrations the process of reduction produced an exothermic heat effect. When the data measured were normalized to the amount of silver ions presented in the solution, the resulting curve showed the molar enthalpy of reduction of silver as a function of the concentration of the reducing agent (Fig. 3b).

On further analysis of our data, the next question to arise was how the precursor/reducing agent ratio affected the enthalpy of Ag particle formation. As shown
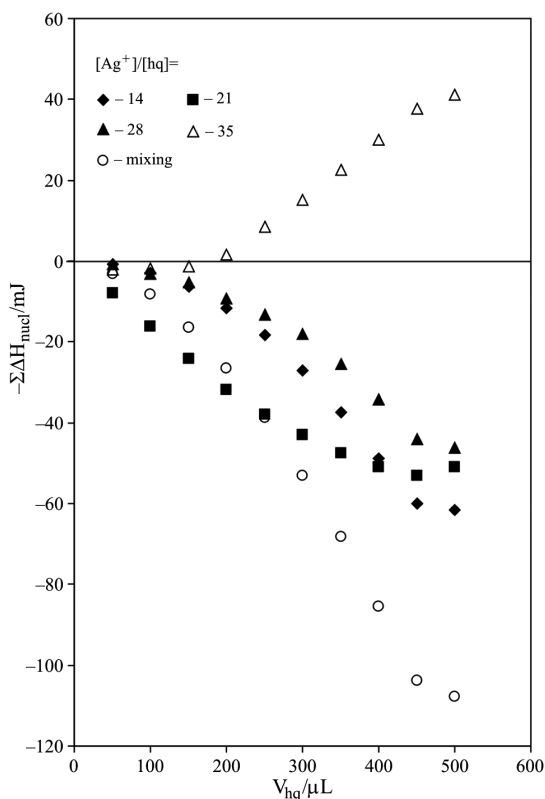
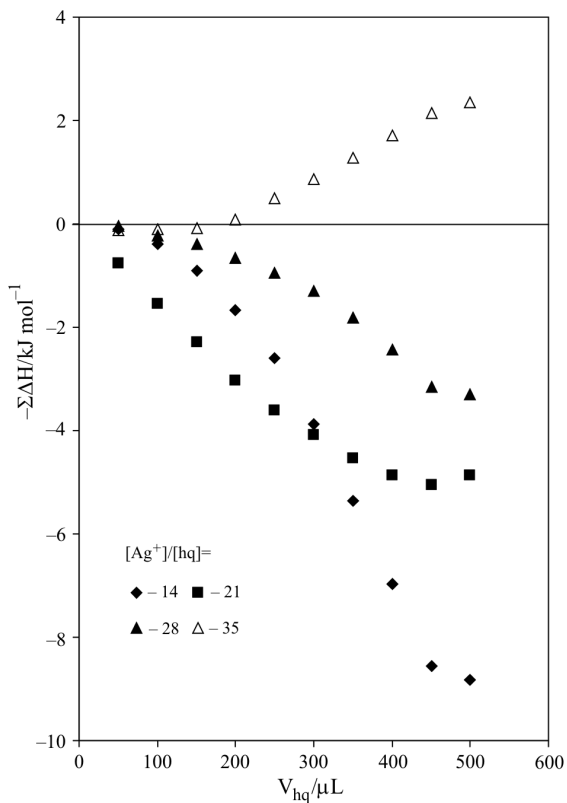**Fig. 3a** The nucleation enthalpy as a function of addition of hq

in Fig. 4, this ratio (whose value varies in the range of 1–35) as a function of Ag^+ precursor concentration had a minimum with increasing Ag^+ precursor concentration and reached into the exothermic range. At precursor/reducing agent ratio=28–35 aggregates of large Ag nanoparticles (particle diameter 15–20 nm) were already formed.

Based on the experimental evidence above, the formation of nanoparticles as monitored by calorimetry can be divided into three stages. In stage 1 silver ions were turned into metallic silver clusters by the effect of the reducing agent, a process that can be considered as nucleation (Fig. 5). In the course of this process silver ions formed silver clusters and concomitantly lost their own hydration shell; in other words, nucleation was associated with the dehydration of silver ions, the enthalpy change of which was endothermic. This heat effect was insignificant; however, the enthalpy requirement of dehydration, 451.9 kJ mol^{-1} [21] also had to be taken into consideration. When the concentration of precursor ions was further increased, nucleation was followed by particle growth and heat effects detectable by calorimetry were shifted to the endothermic direction. Thus, at this stage Ag^+ ions adsorbed on the surface of Ag clusters were reduced and particle size further increased. This was also demonstrated by the UV-Vis absorption spectra recorded
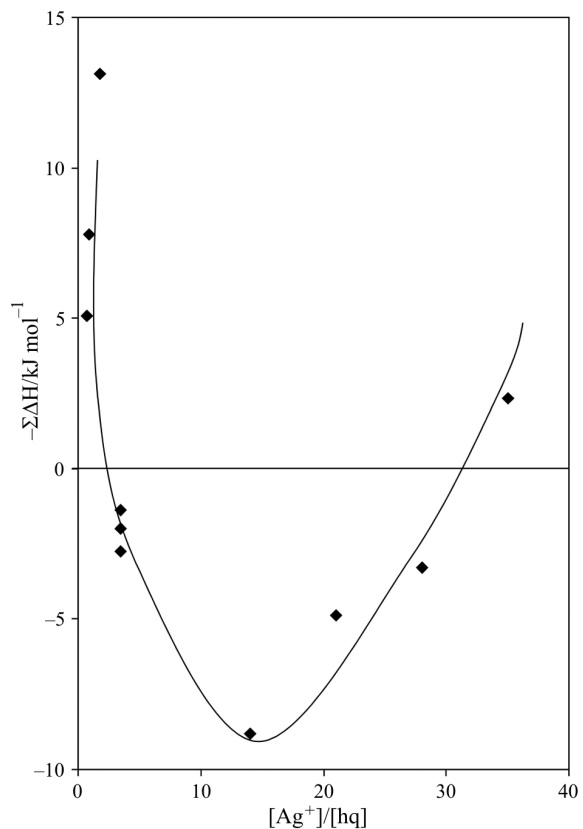

Fig. 3b The molar enthalpy of reduction of silver nanoparticles as a function of the reducing agent

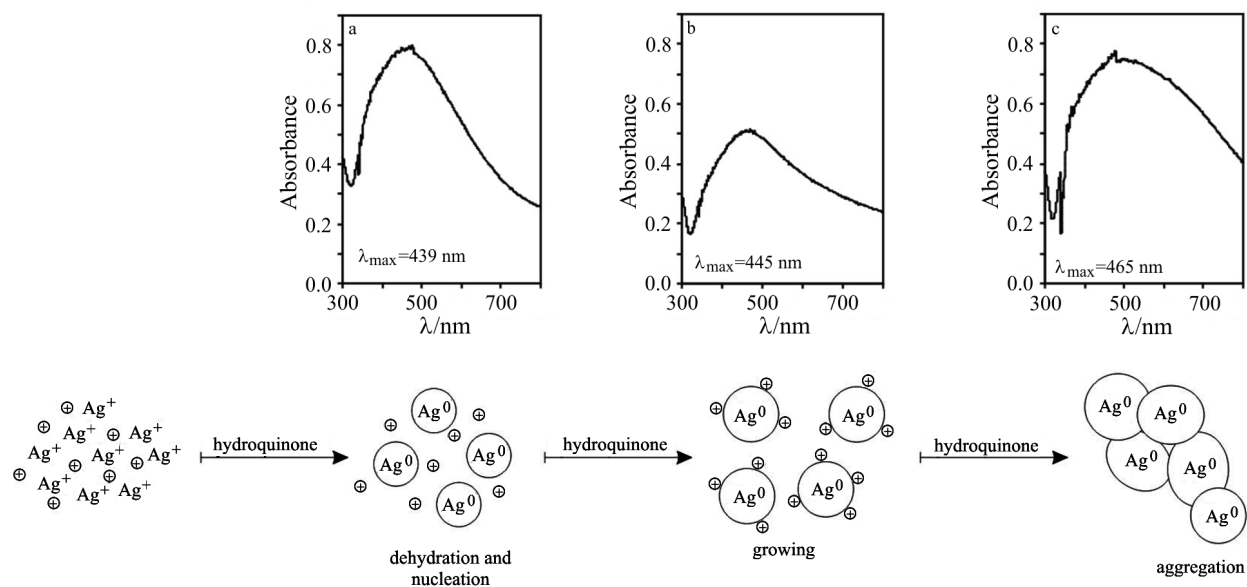**Fig. 4** The molar enthalpy as a function of the [Ag$^+$]/[hq] ratio

Fig. 5 Schematic picture and UV-Vis spectra of the formation of silver nanoparticles (a – $[Ag^+]/[hq]=14$, b – $[Ag^+]/[hq]=21$, c – $[Ag^+]/[hq]=35$)
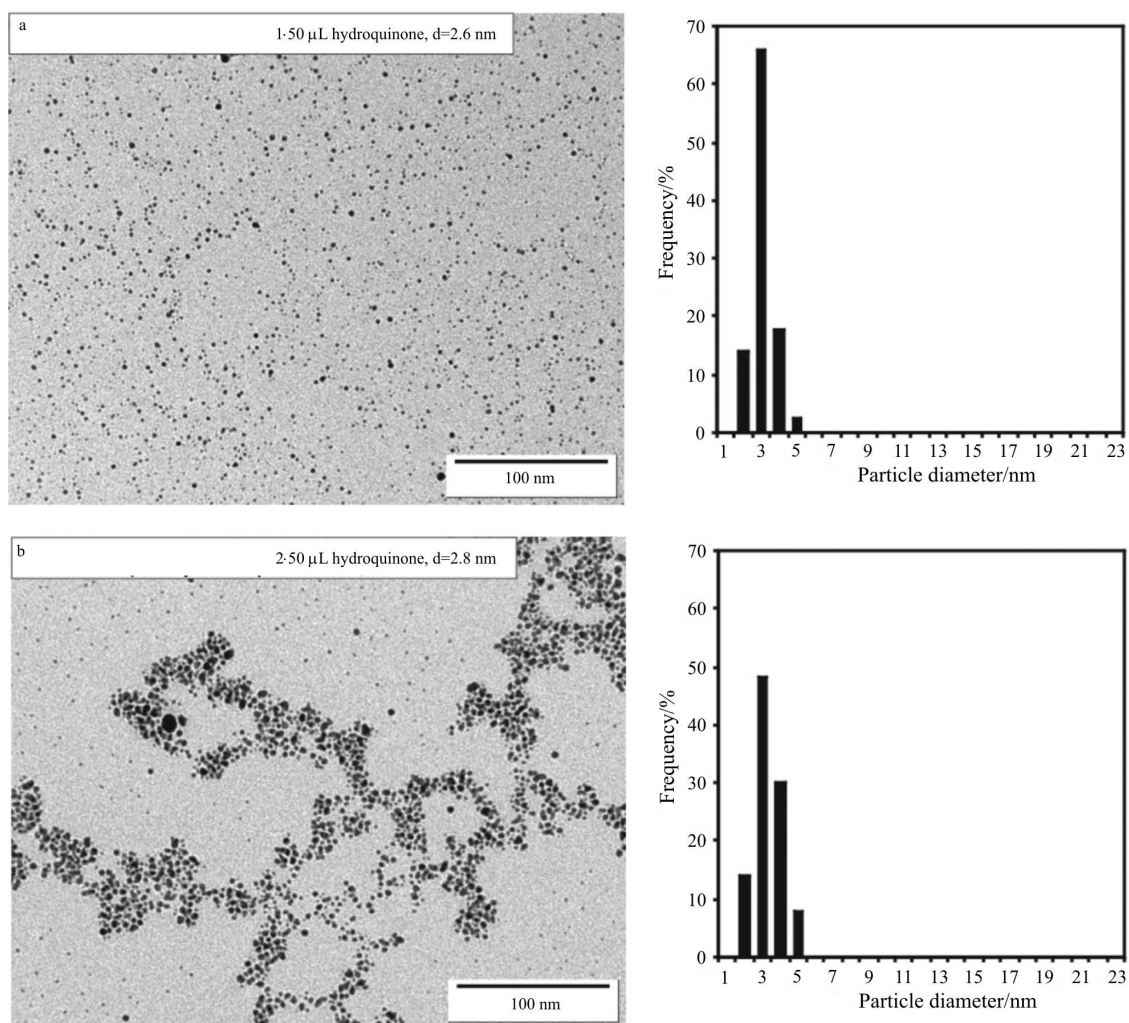

Fig. 6 TEM images and size distributions of silver nanoparticles during the synthesis at different time and added hydroquinone volume ($[Ag^+]/[hq]=35$, $10\cdot 50\ \mu L$ 1 mM hydroquinone solution is added to 1.75 mL 10 mM $AgNO_3$ and 0.25 mL 10 mM Na citrate)
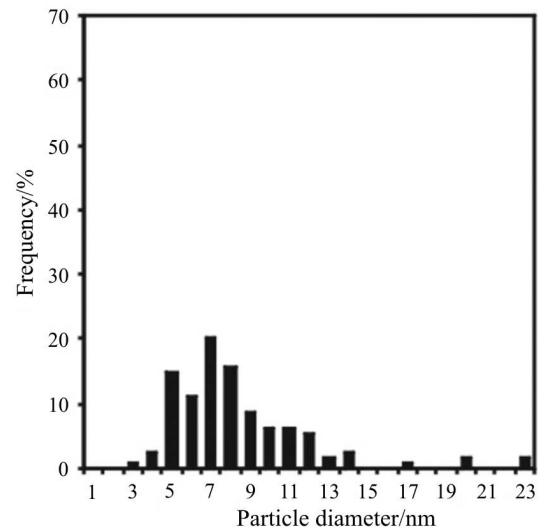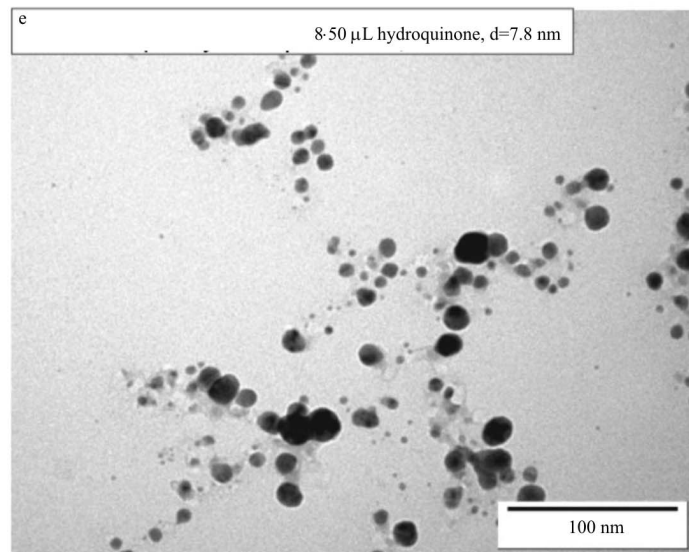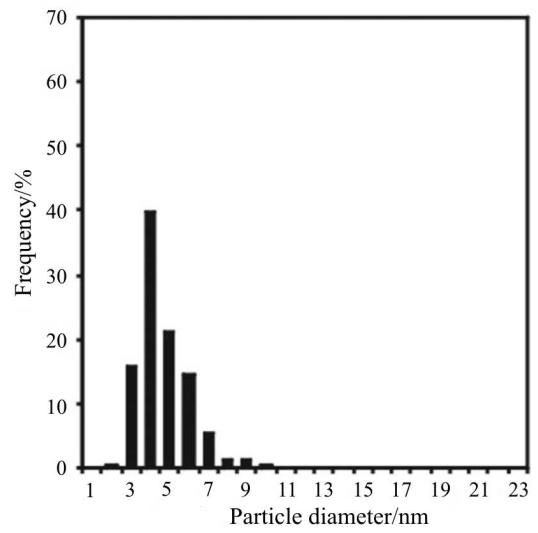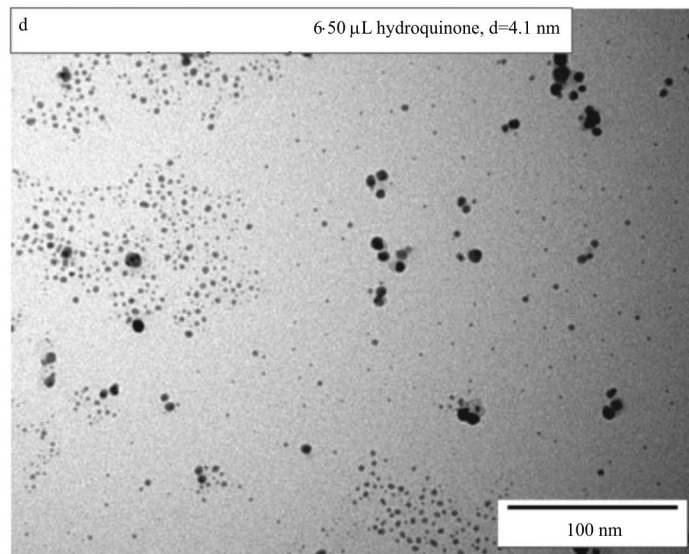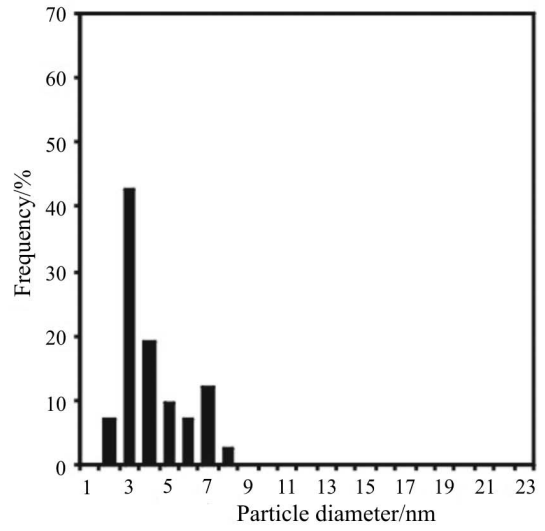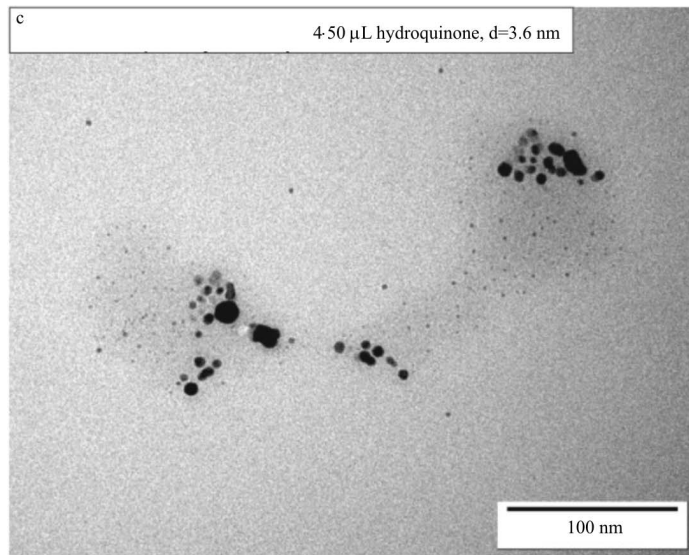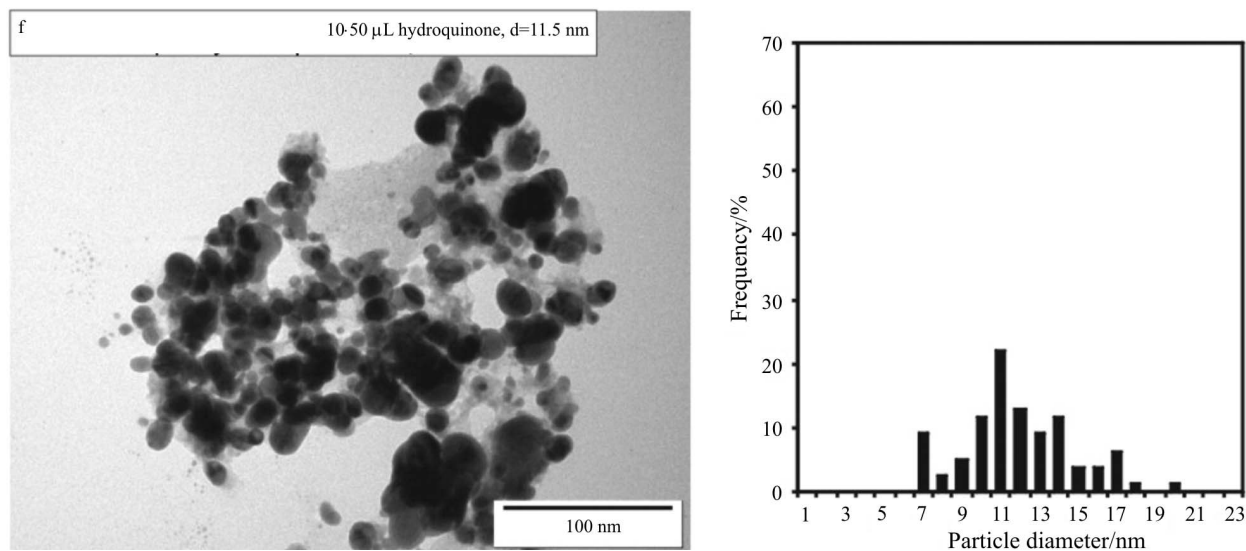
Fig. 6 Continued

Fig. 6 Continued

reveal that at Ag concentrations of 2–4 mM a relatively sharp absorption maximum appeared at λ=439 nm, indicating the formation of small, nearly monodisperse particles (a). The growth of particles at increased Ag^+ concentrations of 6–8 mM was shown by the absorption spectra determined in parallel measurements (b). The broadening of the spectra and the shift of the absorption maximum (λ=445 nm) were proof for particle growth, which was accompanied by an endothermic heat effect. When the Ag/hydroquinone ratio was further increased, the particles began to aggregate in spite of the fact that in every case the stabilizer Na-citrate was present in the solution (c, λ=465 nm). Coagulation of Ag particles leading to the appearance of larger aggregates causes heat release, the process was exothermic, which means that this effect again overcompensated the endothermic effect associated with the dehydration of the large amount of Ag^+ ions present (10 mM). The processes of nucleation, particle growth and aggregation brought about by the addition of the reducing agent hydroquinone can be observed within a given experimental sequence. In Fig. 6 transmission electron micrographs of particle size distributions in the sol containing 10 mM of Ag^+ precursor were displayed. Nucleation dominated after the addition of up to 2·50 μL hydroquinone and the average particle diameter was d=2.6 nm (Fig. 6a). Next, the addition of 6·50 μL hydroquinone initiated particle growth and d=4.1 nm (Fig. 6d). After the addition of 8·50 μL reducing agent, the particles were aggregated and d=7.8 nm (Fig. 6e).

Conclusions

The nucleation and growth of silver nanoparticles was followed in a titration microcalorimeter as well as by spectrophotometry and transmission electron micros-copy. The silver ion/hydroquinone ratios (concentration ranges) at which nucleation, particle growth and the subsequent aggregation of nanoparticles take place were identified with the help of spectrophotometry and TEM and the heat effects determined by microcalorimetry were assigned to them.

Acknowledgements

References

1 N. R. Jana, Z. L. Wang and T. Pal, Langmuir, 16 (2000) 2457.
2 M. Brust and C. J. Kiely, Colloids Surf., A, 202 (2002) 175.
3 S. Y. Kang and K. Kim, Langmuir, 14 (1998) 226.
4 M. Y. Han and C. H. Quek, Langmuir, 16 (2000) 362.
5 S. Papp and I. Dékány, Colloid. Polym. Sci., 279 (2001) 449.
6 P. C. Lee and D. Miesel, J. Phys. Chem., 86 (1982) 3391.
7 J. A. Creighton, C. G. Blatchford and M. G. Albrecht, Trans. Faraday Soc., 75 (1979) 790.
8 L. Quaroni and G. Chumanov, J. Am. Chem. Soc., 121 (1999) 10642.
9 I. Pastoriza-Santos and L. M. Liz-Marzán, Langmuir, 15 (1999) 948.
10 J. J. Zhu, Q. F. Qiu, H. Wang, J. R. Zhang, J. M. Zhu and Z. Q. Chen, Inorg. Chem. Commun., 5 (2002) 242.
11 W. C. Bell and M. L. Myrick, J. Colloid Interface Sci., 242 (2001) 300.
12 J. A. Creighton and D. G. Eadon, J. Chem. Soc. Faraday Trans., 87 (1991) 3881.
13 H. S. Kim, J. H. Ryu, B. Jose, B. G. Lee, B. S. Ahn and Y. S. Kang, Langmuir, 17 (2001) 5817.
14 D.-W. Kim, S.-I. Shin and S.-G. Oh, Surfactant Sciences Series, Marcel Dekker, New York Basel 2003, p. 255.

15 S. A. Vorobyova, N. S. Sobal and A. I. Lesnikovich,
   Colloids Surf., A, 176 (2001) 273.
16 N. Shirtcliffe, U. Nickel and S. Schneider,
   J. Colloid Interface Sci., 211 (1999) 122.
17 D'Aprano, I. D. Donato, F. Pinio and V. Turco Liveri,
   J. Solution Chem., 19 (1990) 589.
18 V. Arcoleo, G. Cavallaro, G. La Manna and V. Turco Liveri,
   Thermochim. Acta, 254 (1995) 111.

19 F. Aliotta, V. Arcoleo, S. Buccoleri, G. La Manna and
   V. Turco Liveri, Thermochim. Acta, 265 (1995) 15.
20 M. L. Turco Liveri and V. Turco Liveri,
   J. Colloid Interface Sci., 176 (1995) 101.
21 D. Dobos, Elektrokémiai táblázatok, Műszaki könyvkiadó,
   Budapest 1979, p. 101.